# Solvent Effects. 2. Medium Effect on the Structure, Energy, Charge Density, and Vibrational Frequencies of Sulfamic Acid

**Ming Wah Wong,[†] Kenneth B. Wiberg,\*,[†] and Michael J. Frisch[‡]**

*Contribution from the Department of Chemistry, Yale University, New Haven, Connecticut 06511, and Lorentzian Inc., 127 Washington Avenue, North Haven, Connecticut 06473.
Received May 8, 1991*

**Abstract:** High-level ab initio molecular orbital studies, using basis sets up to 6-31+G(2d,p), with electron correlation included at the second-order Møller–Plesset perturbation level, are reported for the geometry, energy, dipole moment, charge distribution, and vibrational frequencies of both the zwitterion ($^+H_3NSO_3^-$) and neutral acid form ($NH_2SO_2OH$) of sulfamic acid in the gas phase and condensed media. In the gas phase, the zwitterion (staggered $C_{3v}$, **1a**) and neutral form (gauche $C_1$, **2a**) lie very close in energy, with the neutral form favored by 0.5 kcal mol$^{-1}$. The interconversion of **1a** and **2a**, via a hydrogen 1,3-shift, is predicted to be separated by a barrier of 28.6 kcal mol$^{-1}$. Thus, both **1a** and **2a** should be experimentally observable in the gas phase. The N–S bond of the zwitterion exhibits the characteristics of a covalent interaction. The calculated covalent bond order (0.46) is significantly larger than that computed for the B–N bond of amine–borane $BH_3\cdot NH_3$ (0.26). Onsager reaction field theory has been applied to investigate the effect of medium on this dipolar molecule. The inclusion of a solvent reaction field has a strong influence on the energies, molecular properties, and IR spectra. Consistent with the experimental observations, the zwitterion is predicted to be strongly favored in a condensed dielectric medium of $\epsilon$ = 40.0, by 10.2 kcal mol$^{-1}$. The N–S bond of the zwitterion is found to be reduced dramatically, by 0.10 Å, on going from the gas phase to a polar medium. The calculated SCRF geometry of the zwitterion is in satisfactory agreement with X-ray structural data. Sizable vibrational frequency shifts and intensity changes for both **1a** and **2a** are calculated on going from the gas phase to a polar medium. The changes in vibrational frequencies are in good accord with the solid-state experimental values.

## Introduction

Sulfamic acid is one of the most widely used inorganic compounds in industry. Its syntheses, industrial uses, physical properties (structural and spectroscopic), and chemical reactions have been extensively reviewed.[1] It is well established that the zwitterionic form, $^+H_3NSO_3^-$ (**1**), is more stable than the neutral acid form, $H_2NSO_2OH$ (**2**), in the solid state.[2] The zwitterionic form has also been conclusively shown to be preferred in aqueous solution[3] and in polar media such as dimethyl sulfoxide.[4] However, little is known about the structure and conformation of sulfamic acid in the gas phase. The structure of both the zwitterion and neutral form have received some theoretical attention in the past.[5] In this paper, we report the characterization of this species through high-level ab initio molecular orbital (MO) calculations. In particular, we ascertain whether or not sulfamic acid is zwitterionic in vacuo.

In a recent paper, Hickling and Woolley[5a] reported theoretical studies of the structure of the zwitterion of sulfamic acid. Their best calculated N–S bond length, 1.95 Å, is found to be considerably longer than the experimental value (1.76 Å) determined from X-ray crystal study.[2d] This raises the question of whether this large difference can be attributed to an inadequate basis set, neglect of electron correlation, or a genuine medium effect. In the present paper, we attempt to answer this intriguing question by performing ab initio calculations at levels significantly higher than those used previously and also examining the effect of medium on the molecular geometry.

Finally, we report the results of the effect of medium on the energy, structure, charge distribution, and vibrational frequencies of this dipolar molecule. The Onsager reaction field theory[6] in the framework of ab initio SCRF formalism[7,8] was employed to include the solute–solvent interaction. Amino acids are structurally related to sulfamic acid as bifunctional compounds. Like sulfamic acid, amino acids exist predominantly as zwitterions in a condensed phase. Hence, the study here may also shed light on the understanding of molecular interactions in these biologically important compounds.

## Theoretical Methods and Results

Standard ab initio MO calculations were performed using a development version of the GAUSSIAN 91 series of programs.[9] To examine the effect of basis set on the structure of sulfamic acid, we have first optimized the molecular geometry of the zwitterion with a sequence of standard basis sets,[10] including 6-31G(d), 6-31G(d,p), 6-31+G(d), 6-31G(2d), 6-31+G(2d), and 6-311G(d), at the Hartree–Fock (HF) level. To investigate further the effect of electron correlation, the geometry of **1a** was also optimized at the second-order Møller–Plesset perturbation (MP2)[11] and configuration interaction with singles and doubles (CISD) theory levels, using the 6-31(d) basis set.

Geometry optimizations for the staggered (**1a**) and eclipsed (**1b**) conformations of zwitterion ($^+H_3NSO_3^-$), the anti (**2a**) and gauche (**2b**) forms with respect to the HOSN torsional plane of the neutral

(1) (a) Audrieth, L. F.; Sveda, M.; Sisler, H. H.; Butler, M. J. *Chem. Rev.* **1940**, *26*, 49. (b) Burton, K. W. C.; Nickless, G. In *Inorganic Sulphur Chemistry*; Nickless, G., Ed.; Elsevier: Amsterdam, 1969; Chapter 18. (c) Benson, G. A.; Spillane, W. J. *Chem. Rev.* **1980**, *80*, 151. (d) Santmeyer, R.; Aarons, R. In *Kirk-Othmer Encyclopedia of Chemical Technology*; Standen, A., Ed.; Interscience: New York, 1969; Vol. 19, p 242.

(2) (a) Kanda, F. A.; King, A. J. *J. Am. Chem. Soc.* **1951**, *73*, 2315. (b) Sass, R. L. *Acta Crystallogr. B* **1960**, *13*, 320. (c) Cameron, A. F.; Duncanson, F. D. *Acta Crystallogr. B* **1976**, *36*, 1563. (d) Bats, J. W.; Coppens, P. Koetzle, T. F. *Acta Crystallogr. B* **1977**, *37*, 1333. (e) Reuven, A.; Marcellus, D.; Parker, R. S.; Kwiram, A. L. *J. Chem. Phys.* **1981**, *74*, 179.

(3) Hopkins, H. P., Jr.; Wu, C. H.; Hepler, L. G. *J. Phys. Chem.* **1965**, *69*, 2244.

(4) (a) Benoit, R. L.; Boulet, D.; Frechette, M. *Can. J. Chem.* **1988**, *66*, 3038. (b) Turner, E. M.; Sears, P. G. *Inorg. Nucl. Chem.* **1973**, *35*, 2087. (c) Hovermale, R. A.; Sears, P. G. *J. Phys. Chem.* **1956**, *60*, 1579.

(5) (a) Hickling, S. J.; Woolley, R. G. *Chem. Phys. Lett.* **1990**, *166*, 43. (b) Kaliannan, P.; Vishveswara, S.; Rao, V. S. R. *J. Mol. Struct.* **1983**, *105*, 359. (c) Kaliannan, P.; Vishveswara, S.; Rao, V. S. R. *Current Sci.* **1987**, *54*, 111. (d) Cruickshank, D. W. J.; Eisentein, M. *J. Mol. Struct.* **1985**, *130*, 143. (e) Douglas, J. E.; Kenyon, G. L.; Kollman, P. A. *Chem. Phys. Lett.* **1978**, *57*, 553.

(6) Onsager, L. *J. Am. Chem. Soc.* **1936**, *58*, 1486.

(7) Wong, M. W.; Frisch, M. J.; Wiberg, K. B. *J. Am. Chem. Soc.*, **1990**, *113*, 4776.

(8) Tapia, O.; Goscinski, O. *Mol. Phys.* **1975**, *29*, 1653.

(9) Frisch, M. J.; Head-Gordan, M.; Trucks, G. W.; Foresman, J. B.; Schlegel, H. B.; Raghavachari, K.; Robb, M. A.; Wong, M. W.; Replogle, E. S.; Binkley, J. S.; Gonzalez, C.; DeFrees, D. J.; Fox, D. J.; Whiteside, R. A.; Seeger, R.; Melius, C. F.; Baker, J.; Martin, R. L.; Kahn, L. R.; Stewart, J. J. P.; Topiol, S.; Pople, J. A. *GAUSSIAN 91*, Development Version, Revision B; Gaussian Inc.: Pittsburgh PA, 1991.

(10) Hehre, W. J.; Radom, L.; Schleyer, P. v. R.; Pople, J. A. *Ab Initio Molecular Orbital Theory*; Wiley: New York, 1986.

(11) (a) Møller, C.; Plesset, M. S. *Phys. Rev.* **1934**, *46*, 618. (b) Pople, J. A.; Binkley, J. S.; Seeger, R. *Int. J. Quantum Chem. Symp.* **1976**, *10*, 1.

[†] Yale University.
[‡] Lorentzian, Inc.

($H_2NSO_2OH$), and the transition structure corresponding to hydrogen 1,3-shift from **1a** to **2a** (**3**) were carried out with the 6-31G(d) and 6-31+G(2d) basis sets at the HF level. Unless otherwise noted, geometric parameters in the text refer to the HF/6-31+G(2d) values. Harmonic vibrational frequencies were calculated analytically at the HF/6-31+G(2d) level in order to characterize stationary points as minima (representing equilibrium structures) or saddle points (representing transition structures) and to evaluate zero-point vibrational energies (ZPVEs). The directly calculated frequencies and ZPVEs were scaled by a factor of 0.9 to allow for the overestimation of vibrational frequencies at the HF level. Improved relative energies were obtained through second-order Møller–Plesset calculations with the larger 6-31+-G(2d,p) basis set based on the HF/6-31+G(2d) optimized geometries. Our best relative energies correspond to MP2/6-31+-G(2d,p)//HF/6-31+G(2d) values with zero-point vibrational corrections. Unless otherwise noted, these are the values given in the text. To obtain a definitive result of the energy difference between the zwitterion and neutral form, we have also performed single-point energy calculations at the MP4SDQ[11] and QCISD[12] levels, using the HF/6-31+G(2d) optimized structures. The frozen-core approximation was employed for the MP4 and QCISD calculations.

To take into account the effect of the medium, we have employed the self-consistent reaction field (SCRF) method in the MO formalism.[7,8] This method is based on Onsager reaction field theory[6] of the electrostatic solute–solvent interaction and has proven to be quite successful in reproducing the solvent effects of rotational and tautomeric equilibria.[7,13] In this reaction field model, the solvent is represented by a continuous dielectric, characterized by a given dielectric constant ($\epsilon$). The solute is assumed to be embedded into a spherical cavity, with radius $a_0$, in the medium. The permanent dipole of the solute will induce a dipole in the medium, which in turn will interact with the molecular dipole to lead to stabilization. In the SCRF MO formalism, the solute–solvent interaction is treated as a perturbation of the Hamiltonian of the isolated molecule. The reaction field is updated iteratively until the intramolecular electric field is self-consistent (cf. ref 7). Note that the solvation energy calculated by the SCRF method is the electrostatic contribution to the free energy of solvation. In the present work, the cavity radius of sulfamic acid ($a_0 = 3.0$ Å) was calculated from the molar volume of the crystal,[14] adding 0.5 Å to account for the nearest approach of solvent molecules. A dielectric constant of 40.0 was used for the SCRF calculations to represent a polar medium. Since sulfamic acid is a relatively compact molecule, the simple spherical cavity is a satisfactory approximation. Full geometry optimizations of all structures of sulfamic acid in a dielectric medium of $\epsilon = 40.0$ were obtained at the HF/6-31+g(2d) level using the SCRF analytic-gradient method.[7] The vibrational frequencies of all the stationary points were also determined using the recently developed analytical method of evaluating second derivatives of Hartree–Fock energy in the presence of a reaction field.[15] For the higher level single-point energy calculations, we have employed the MP2 theory to incorporate the effect of electron correlation.

In order to gain further information for **1a**, **2a**, and some related species, we have carried out a quantum topological analysis.[16] We studied the topological parameters of the charge density and its Laplacian. The electron populations were derived by numerical integration of the charge densities, using the boundary conditions derived by Bader's theory of atoms in molecules.[16] The charge

(12) Pople, J. A.; Head-Gordon, M.; Raghavachari, K. *J. Chem. Phys.* **1987**, *87*, 5968.

(13) Wong, M. W.; Wiberg, K. B.; Frisch, M. J. *J. Am. Chem. Soc.*, submitted for publication.

(14) *The Merck Index*; Winholz, M. Ed.; Merck & Co.: Rahway, NJ, 1983.

(15) Wong, M. W.; Wiberg, K. B.; Frisch, M. J. *J. Chem. Phys.*, submitted for publication.

(16) (a) Bader, R. F. W. *Acc. Chem. Res.* **1985**, *9*, 18. (b) Bader, R. F. W. *Atoms in Molecules. A Quantum Theory*; Oxford University Press: New York, 1990.

**Table I.** Optimized Geometries for the Zwitterion (**1a**) of Sulfamic Acid

| level | $r$(N–S) | $r$(S–O) | $r$(N–H) | ∠OSN | ∠HNS |
|---|---|---|---|---|---|
| | | Gas Phase | | | |
| HF/STO-3G[a] | 2.567 | 1.600 | 1.032 | 94.8 | 113.7 |
| HF/3-21G[a] | 2.046 | 1.541 | 1.012 | 96.6 | 108.2 |
| HF/3-21G(d)[a,b] | 1.960 | 1.421 | 1.012 | 97.2 | 108.7 |
| HF/6-31G(d) | 1.950 | 1.418 | 1.007 | 97.5 | 109.7 |
| HF/6-31G(d,p) | 1.949 | 1.419 | 1.005 | 97.6 | 109.5 |
| HF/6-311G(d) | 1.954 | 1.411 | 1.002 | 97.6 | 109.6 |
| HF/6-31+G(d) | 1.931 | 1.420 | 1.007 | 97.8 | 109.8 |
| HF/6-31G(2d) | 1.937 | 1.405 | 1.005 | 97.5 | 109.3 |
| HF/6-31+G(2d) | 1.912 | 1.407 | 1.005 | 97.8 | 109.3 |
| MP2/6-31G(d) | 2.081 | 1.457 | 1.021 | 96.2 | 109.5 |
| CISD/6-31G(d) | 1.972 | 1.434 | 1.014 | 97.2 | 109.5 |
| | | Condensed Media[c] | | | |
| HF/6-31G(d)[d] | 1.893 | 1.422 | 1.009 | 98.9 | 110.2 |
| HF/6-31G(d)[e] | 1.836 | 1.428 | 1.013 | 101.1 | 111.3 |
| HF/6-31+G(2d)[e] | 1.817 | 1.415 | 1.012 | 101.0 | 110.9 |
| experiment[f] | 1.76 | 1.44 | 1.02 | 103.0 | 111.0 |

[a] Taken from ref 5a. [b] d-Polarization functions on second-row atoms only. [c] SCRF calculations ($a_0 = 3.0$ Å). [d] $\epsilon = 2.0$. [e] $\epsilon = 40.0$. [f] From ref 2d.
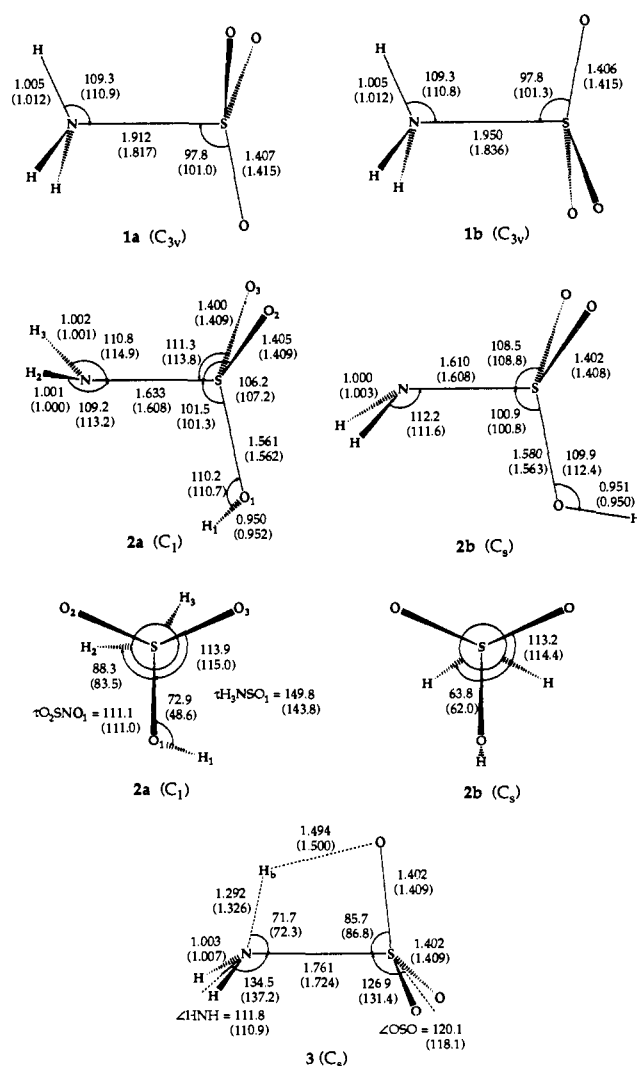


**Figure 1.** Optimized geometries (gas-phase values ($\epsilon = 1.0$) with condensed-phase ($\epsilon = 40.0$) values in parentheses) of the zwitterions (**1a**, **1b**), neutral forms (**2a**, **2b**), and transition structure (**3**) of sulfamic acid.

densities were obtained from the HF/6-31+G(2d,p) calculations based on the HF/6-31+G(2d) optimized geometries. At the bond critical points we calculated $\rho_b$, the electronic density, $\nabla^2\rho_b$, the Laplacian of the density which is a measure of the concentration

**Table II.** Total Energies (Hartrees), Dipole Moments (D), and Zero-Point Vibrational Energies (ZPVE, kcal mol⁻¹) for Sulfamic Acid and Related Species

| species | symmetry | $N_i^a$ | total energy[b,c] HF/6-31G(d) | HF/6-31+G(2d) | MP2/6-31+G(2d,p)[f] | dipole[c,d] | ZPVE[e] |
|---|---|---|---|---|---|---|---|
| staggered ⁺NH₃SO₃⁻ (1a) | $C_{3v}$ | 0 | −678.204 02 (−678.232 47) | −678.251 42 (−678.279 97) | −679.287 49 (−679.313 09) | 6.61 (9.69) | 35.88 (35.99) |
| eclipsed ⁺NH₃SO₃⁻ (1b) | $C_{3v}$ | 1 | −678.201 97 (−678.230 44) | −678.248 96 (−678.277 50) | −679.286 21 (−679.311 55) | 6.50 (9.74) | 35.39 (35.61) |
| gauche NH₂SO₃H (2a) | $C_1$ | 0 | −678.210 30 (−678.221 93) | −679.256 62 (−678.266 80) | −679.284 97 (−679.294 67) | 3.56 (5.89) | 34.95 (34.45) |
| anti NH₂SO₃H (2b) | $C_s^g$ | 0 | −678.210 20 (−678.224 51) | −679.256 22 (−678.264 62) | −679.284 69 (−679.291 74) | 3.61 (4.89) | 34.63 (34.32) |
| TS: 1a → 2a (3) | $C_s$ | 1 | −678.139 70 (−678.158 19) | −679.188 12 (−678.205 80) | −679.237 03 (−679.252 39) | 5.21 (7.19) | 32.43 (32.14) |
| SO₃ | $C_{3v}$ | 0 | −621.981 57 (−621.981 57) | −622.028 28 (−622.028 28) | −622.834 24 (−622.834 24) | 0.00 (0.00) | 8.63 (8.63) |
| NH₃ | $C_{3v}$ | 0 | −56.184 36 (56.188 71) | −56.191 78 (−56.195 52) | −56.416 62 (−56.420 52) | 1.73 (2.35) | 22.90 (22.90) |

*[a]* Number of imaginary frequencies. *[b]* Geometries fully optimized at the level specified, unless otherwise noted. *[c]* SCRF values ($\epsilon$ = 40.0) in parentheses. $a_0$ values for sulfamic acid and NH₃ are 3.0 and 2.2 Å, respectively. *[d]* MP2/6-31+G(2d,p) values. *[e]* Unscaled HF/6-31+G(2d) values. *[f]* Based on HF/6-31+-G(2d) optimized geometries. *[g]* $C_1$ symmetry at HF/6-31G(d) level.

**Table III.** Relative Energies (kcal mol⁻¹) of Sulfamic Acid[a]

| species | HF/6-31G(d) | | HF/6-31+G(2d) | | MP2/6-31+G(2d,p) | | MP2/6-31+G(2d,p)[b] | |
|---|---|---|---|---|---|---|---|---|
| staggered ⁺H₃NSO₃⁻ (1a) | 0 | (0) | 0 | (0) | 0 | (0) | 0 | (0) |
| eclipsed ⁺H₃NSO₃⁻ (1b) | 1.29 | (1.27) | 1.54 | (1.55) | 0.80 | (0.97) | 0.36 | (0.63) |
| gauche H₂NSO₃H (2a) | −3.94 | (6.61) | −3.26 | (8.26) | 1.58 | (11.56) | 0.74 | (10.17) |
| anti H₂NSO₃H (2b) | −3.88 | (4.99) | −3.01 | (9.63) | 1.76 | (13.40) | 0.63 | (11.90) |
| TS: 1a → 2a (3) | 40.36 | (46.61) | 39.72 | (46.54) | 31.66 | (38.09) | 28.55 | (34.62) |
| NH₃ + SO₃ | 23.90 | (39.02) | 19.68 | (35.25) | 22.99 | (36.60) | 19.07 | (32.59) |

*[a]* Based on calculated total energies from Table II. *[b]* Includes (scaled) zero-point vibrational energies correction.
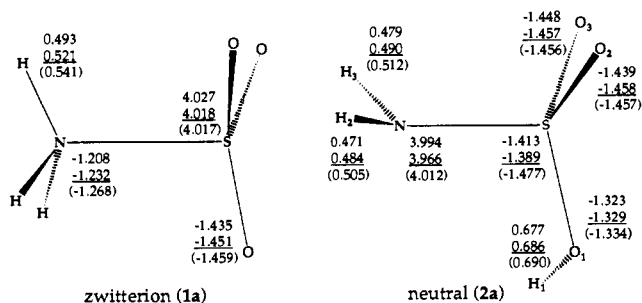


**Figure 2.** Atomic charges of **1a** and **2a** (calculated at the HF/6-31+G-(2d,p) level). The SCRF values evaluated using the gas-phase geometry are underlined, and those using the relaxed SCRF geometry are in parentheses.
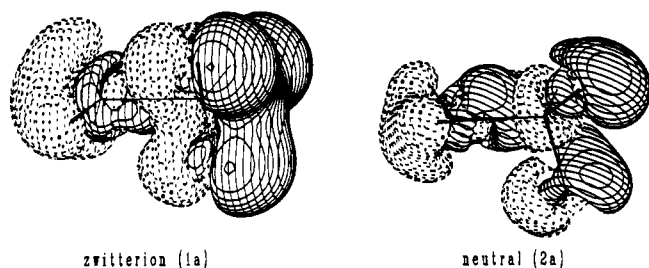


**Figure 3.** Charge density difference plots for **1a** and **2a** on going from the gas phase to a polar medium (using the same gas-phase geometry). The nitrogen atom is shown to the left and the SO₃ group to the right. The contour level is 5 × 10⁻⁴ e/B³.

or depletion of electronic charge, $H_b$, the local energy density ($H_b$ = $G_b$ + $V_b$, i.e., sum of kinetic and potential energy densities), and $\epsilon^* = \lambda_1/(\lambda_2 - 1)$, the bond ellipticity (where $\lambda_1$ and $\lambda_2$ are the major and minor curvatures perpendicular to the bond line). In addition, covalent bond orders were evaluated by a scheme recently proposed by Cioslowski and Mixon.[17] This new scheme is based on the atomic overlap matrix as defined in the theory of atoms in molecules. The analysis of the wave functions was carried out with PROAIM program.[18] The bond orders were calculated using BONDER.[17]

The results of the geometry optimizations are summarized in Table I and Figure 1. The total energies and the dipole moments
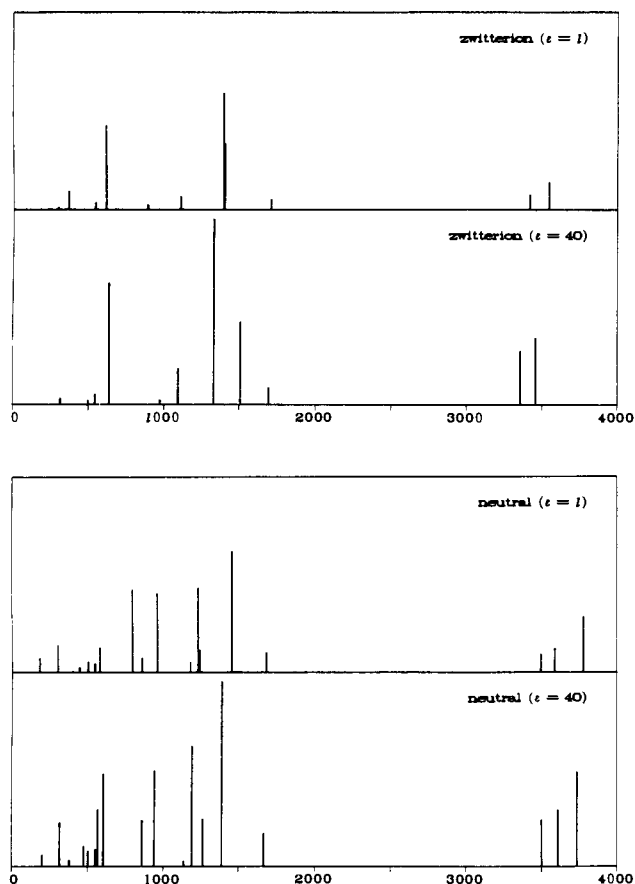


**Figure 4.** Compound IR spectra of **1a** and **2a**. Top half corresponds to the gas phase ($\epsilon$ = 1.0), and bottom half corresponds to the condensed medium ($\epsilon$ = 40.0).

of the sulfamic acid and related systems are given in Table II, and the corresponding relative energies in Table III. The calculated energy differences between **1a** and **1b** are presented in Table IV. The topological quantities calculated at bond critical points are summarized in Table V, and the calculated atomic charges are presented in Figure 2. Finally, vibrational frequencies of **1a** and **2a** are summarized in Tables VI and VII, and the corresponding IR spectra are given in Figure 4. Throughout this

(17) Cioslowski, J.; Mixon, S. T. *J. Am. Chem. Soc.* **1991**, *113*, 4142.
(18) Biegler-Konig, F. W.; Bader, R. F. W.; Tang, T.-H. *J. Comput. Chem.* **1982**, *3*, 317.

**Table IV.** Calculated Total Energies[a] (Hartree) and Relative Energies (kcal mol$^{-1}$) of **1a** and **2a** in the Gas Phase

| | total energy | | |
|---|---|---|---|
| level | zeitterion (**1a**) | neutral form (**2a**) | relative energy |
| HF/6-31G(d)[b] | −678.204 02 | −678.210 30 | −3.94 |
| HF/6-31+G(2d) | −678.251 42 | −678.256 62 | −3.26 |
| HF/6-31+G(2d,p) | −678.263 99 | −678.272 72 | −5.48 |
| HF/6-31+G(2df,p) | −678.302 17 | −678.311 10 | −5.60 |
| HF/6-311+G(2d,p) | −678.361 79 | −678.370 78 | −5.64 |
| MP2/6-31+G(2d,p) | −679.287 49 | −679.284 97 | 1.58 |
| MP3/6-31+G(2d,p)[c] | −679.221 35 | −679.224 07 | −1.71 |
| MP4DQ/6-31+G(2d,p)[c] | −679.224 80 | −679.226 82 | −1.27 |
| MP4SDQ/6-31+G(2d,p)[c] | −679.237 98 | −679.238 83 | −0.53 |
| QCISD/6-31+G(2d,p)[c] | −679.238 00 | −679.239 22 | −0.77 |
| QCISD(T)/6-31+G(2d,p)[c,d] | | | 0.35 |
| QCISD(T)/6-31+G(2d,p)[c,e] | | | −0.49 |

[a] Energy evaluated at the HF/6-31+G(2d) optimized geometry, unless otherwise noted. [b] Based on HF/6-31G(d) optimized geometry. [c] Frozen-core approximation. [d] Includes the zero-point vibrational energy correction (−0.84 kcal mol$^{-1}$). [e] Effect of triple excited configurations (1.12 kcal mol$^{-1}$) is estimated from QCISD(T)/6-31G(d) calculations.

paper, bond lengths are given in angstroms and bond angles in degrees.

## Structural Comparison

The structure of the zwitterion of sulfamic acid (**1a**) has been studied recently by Hickling and Woolley, using ab initio MO calculations.[5a] Their main conclusion was that this dipolar species requires an extended basis set containing polarization functions for a reasonable description of the molecular geometry. However, their best theoretical estimate of the N–S bond length (1.95 Å, obtained from a partial optimization at the HF/6-31(d,p) level) is still substantially longer than the reported solid-state value (1.76 Å). In order to resolve this discrepancy, we have considered here the effects of basis set, full geometry optimization, electron correlation, and medium on this zwitterion.

The molecular structure of the zwitterion (**1a**) was optimized at the Hartree–Fock level, with the 6-31G(d), 6-31G(d,p), 6-31+G(d), 6-31G(2d), 6-31+G(2d), and 6-311G(d) basis sets.[10] The smaller basis set results of previous studies are also included in Table I. It can be seen that the variations in N–H bond length and the OSN and HNS bond angles calculated at various levels

of theory are generally small. The largest effect appears to be associated with the N–S bond length. Significant changes occur on going from 6-31G(d) to 6-31+G(d), i.e., inclusion of diffuse sp functions on heavy atom, and from 6-31G(d) to 6-31G(2d), i.e., expanding the basis set from one set of d-polarization functions to two. In both cases, the S–N bond length is significantly reduced (by 0.019 and 0.013 Å, respectively). The effects of p-polarization functions on hydrogen atoms (6-31G(d) → 6-31G(d,p)) and increasing the basis set from double-$\zeta$ valence to triple-$\zeta$ valence (6-31G(d) → 6-311G(d)) are very small. Thus, it appears that the 6-31+G(2d) basis set should be suitably reliable for structural predictions for the zwitterion and related species.

Large structural changes are observed on going from HF to correlated levels (MP2 and CISD), involving the lengthening of both the N–S and S–O bond lengths. However, the geometry changes between HF and CISD are considerably smaller than those between HF and MP2. Therefore, geometry optimization with the inclusion of electron correlation should be important for more accurate prediction. However, post-HF geometry optimizations employing the 6-31+G(2d) basis set were not feasible, and we have used the HF/6-31+G(2d) level for structural optimization for other related systems. Assuming additivity of the effects of electron correlation and basis sets, our best estimate of the N–S bond length is 1.93 Å. This value is still substantially longer than the solid-state experimental value of 1.76 Å.

The effect of medium on the molecular geometry of the zwitterion was investigated by Onsager reaction field theory. The geometry of **1a** was optimized with $\epsilon$ = 2.0 (corresponding to nonpolar medium) and $\epsilon$ = 40.0 (polar medium), using the 6-31G(d) basis set. As evident in Table I, the solvent reaction field has a strong influence on the molecular geometry. The calculated N–S bond length is shortened by 0.06–0.11 Å from the gas phase to condensed media. The OSN bond angles are also found to widen considerably in a polar medium ($\epsilon$ = 40.0). Larger basis set (6-31+G(2d)) optimization confirms this remarkable change in geometry from the gas phase to condensed media. The SCRF optimized parameters are in reasonable agreement with the solid-state experimental data. Hence, we may conclude that the large discrepancy between the calculated N–S bond length of the zwitterion in the gas phase and that reported from the X-ray crystal structure can be attributed to the medium effect in the molecular geometry. There is also evidence for a similar medium effect on the N–S bond length of the trimethylamine–sulfur dioxide complex ($(CH_3)_3N–SO_2$). The N–S bond length of this

**Table V.** Topological Properties (au) at the Bond Critical Point[a]

| molecule ($\epsilon$) | bond | $\rho_b$ | $\nabla^2\rho_b$ | $H_b$ | bo[b] | $\epsilon^{*c}$ |
|---|---|---|---|---|---|---|
| zwitterion (**1a**) (1.0) | N–S | 0.127 | −0.073 | −0.0810 | 0.463 | 0.000 |
| zwitterion (**1a**) (40.0)[d] | N–S | 0.135 | −0.119 | −0.0872 | 0.529 | 0.000 |
| zwitterion (**1a**) (40.0) | N–S | 0.163 | −0.254 | −0.1392 | 0.584 | 0.000 |
| neutral (**2a**) (1.0) | N–S | 0.252 | −0.686 | −0.3300 | 0.809 | 0.092 |
| neutral (**2a**) (40.0)[d] | N–S | 0.256 | −0.744 | −0.3290 | 0.847 | 0.150 |
| neutral (**2a**) (40.0) | N–S | 0.263 | −0.670 | −0.3589 | 0.828 | 0.127 |
| $BH_3 \cdot NH_3$ (1.0) | B–N | 0.094 | 0.423 | −0.0574 | 0.258 | 0.000 |

[a] Calculated at the SCRF/6-31+G(2d,p) level. [b] Covalent bond order. [c] Ellipticity. [d] Based on the gas-phase geometry.

**Table VI.** Vibrational Frequencies (cm$^{-1}$) for the Zwitterion (**1a**) of Sulfamic Acid

| mode | | SCRF/6-31+G(2d) | | | scaled[b] | | | |
|---|---|---|---|---|---|---|---|---|
| | | $\epsilon$ = 1.0 | $\epsilon$ = 40.0 | shift[a] | $\epsilon$ = 1.0 | $\epsilon$ = 40.0 | obsd[c] | assignment[d] |
| A$_1$ | $\nu_1$ | 3597.7 | 3532.5 | −65.2 | 3238 | 3179 | 3140[e] | sym $NH_3$ stretch |
| | $\nu_2$ | 1473.1 | 1588.0 | 114.9 | 1326 | 1429 | 1445 | sym $NH_3$ deformation |
| | $\nu_3$ | 1166.7 | 1152.1 | −14.6 | 1050 | 1037 | 1066 | sym $SO_3$ stretch |
| | $\nu_4$ | 645.3 | 672.0 | 26.7 | 580 | 605 | 688 | N–S stretch |
| | $\nu_5$ | 383.9 | 525.4 | 141.5 | 346 | 473 | 534 | sym $SO_3$ deformation |
| A$_2$ | $\nu_6$ | 188.0 | 187.5 | −0.5 | 169 | 169 | | hindered rotation about N–S |
| E | $\nu_7$ | 3731.2 | 3639.0 | −92.2 | 3358 | 3275 | 3200[e] | asym $NH_3$ stretch |
| | $\nu_8$ | 1799.2 | 1783.6 | −15.6 | 1619 | 1605 | 1540 | asym $NH_3$ deformation |
| | $\nu_9$ | 1469.9 | 1402.8 | −67.1 | 1323 | 1263 | 1310 | asym $SO_3$ stretch |
| | $\nu_{10}$ | 937.7 | 1026.7 | 89.0 | 844 | 924 | 1003 | asym $NH_3$ rock |
| | $\nu_{11}$ | 570.2 | 573.6 | 3.4 | 513 | 516 | 534 | asym $SO_3$ deformation |
| | $\nu_{12}$ | 311.9 | 334.0 | 22.2 | 281 | 301 | 374 | asym $SO_3$ rock |

[a] Frequency shift from $\epsilon$ = 1.0 to $\epsilon$ = 40.0. [b] Scaled by 0.9. [c] Taken from ref 26a. [d] For a dielectric medium of $\epsilon$ = 40.0. [e] Taken from ref 26b.

*Medium Effects on Sulfamic Acid*

*J. Am. Chem. Soc., Vol. 114, No. 2, 1992* 527

**Table VII.** Vibrational Frequencies[a] (cm⁻¹) for the Neutral Form (**2a**) of Sulfamic Acid

| mode | | $\epsilon = 1.0$ | $\epsilon \approx 40.0$ | shift[b] |
|---|---|---|---|---|
| A | $\nu_1$ | 3974.8 | 3930.1 | −44.7 |
| | $\nu_2$ | 3775.8 | 3797.9 | 22.1 |
| | $\nu_1$ | 3679.4 | 3685.8 | 6.4 |
| | $\nu_4$ | 1772.4 | 1754.9 | −17.5 |
| | $\nu_5$ | 1533.2 | 1463.8 | −69.4 |
| | $\nu_6$ | 1310.5 | 1330.9 | 20.4 |
| | $\nu_7$ | 1296.2 | 1254.4 | −41.8 |
| | $\nu_8$ | 1241.9 | 1196.8 | −41.9 |
| | $\nu_9$ | 1010.7 | 990.0 | −20.7 |
| | $\nu_{10}$ | 903.4 | 904.6 | 1.2 |
| | $\nu_{11}$ | 836.5 | 635.1 | −201.4 |
| | $\nu_{12}$ | 608.8 | 595.5 | −13.3 |
| | $\nu_{13}$ | 574.2 | 578.6 | 4.4 |
| | $\nu_{14}$ | 527.4 | 529.4 | 2.0 |
| | $\nu_{15}$ | 466.8 | 498.8 | 32.0 |
| | $\nu_{16}$ | 422.0 | 402.2 | −19.8 |
| | $\nu_{17}$ | 318.4 | 334.5 | 16.6 |
| | $\nu_{18}$ | 193.2 | 213.1 | 19.9 |

[a] Calculated at the SCRF/6-31+G(2d) level. [b] Frequency shift from $\epsilon = 1.0$ to $\epsilon = 40.0$.

complex in the crystal is 0.2 Å shorter than that in the gas phase, as determined by microwave microscopy.[19] Another remarkable example of medium effect on geometry is given by the amine–borane complex. In a very recent combined experimental/theoretical study of $BH_3 \cdot NH_3$, Bühl et al. have reported a similar inconsistency between the gas-phase and solid-state geometry.[20] The B–N separation in the X-ray crystal structure (1.564 Å)[20] is 0.1 Å shorter than the gas-phase value determined by microwave spectroscopy (1.657 Å).[21] This substantial change in B–N bond length was confirmed by partial geometry optimizations of the $BH_3 \cdot NH_3$ complex in the presence of a reaction field.

Finally, we note that intermolecular hydrogen bonding is important in the crystalline state of sulfamic acid. The measured N–H···O distances in the crystal are 1.95–2.00 Å.[2b] This specific intermolecular interaction in the solid state may lead to a further shortening of the N–S bond of the zwitterion.

## Structures and Energies in the Gas Phase

We have examined both the staggered (**1a**, $C_{3v}$) and eclipsed (**1b**, $C_{3v}$) conformations of the zwitterion. At our best level of theory, the staggered conformation is preferred to the eclipsed conformation by just 0.4 kcal mol⁻¹. The staggered conformation is a true local minimum (with all positive frequencies), whereas the eclipsed conformation is a transition structure (with one imaginary frequency) corresponding to the rotation about the N–S bond. This small rotation barrier suggests that the zwitterion rotates almost freely about the N–S bond. Note that rotation about the N–S bond has a significant effect on the N–S bond length, with the calculated N–S bond length in the eclipsed form being 0.038 Å longer than the staggered form (Figure 1).

The zwitterionic form of sulfamic acid can be considered as a donor–acceptor adduct of ammonia with sulfur trioxide. The N–S bond in this molecule results from the donation of the lone pair electrons of ammonia to the empty $3p_z$ orbital of sulfur trioxide. Previous calculations by Douglas et al. suggested that this interaction represents the strongest known donor–acceptor interaction involving a neutral, second-row Lewis acid.[5c] The heat of reaction for the process $^+H_3NSO_3^-$ (**1a**) → $NH_3 + SO_3$ is calculated to be 19.1 kcal mol⁻¹. Further inclusion of electron correlation, at QCISD level, leads to a slightly smaller value of 16.8 kcal mol⁻¹. This large interaction energy confirms the suggestion that $NH_3$ reacts with $SO_3$ to form a strong donor–

acceptor complex. Experimentally this reaction provides the way of preparing sulfamic acid in industry.

For the neutral acid form ($NH_2SO_2OH$, **2**), two conformations, the gauche (**2a**, $C_1$) and anti (**2b**, $C_s$) conformations with respect to HOSN torsional plane, were considered. Figure 1 presents the optimized structures as well as the Newman projections of the two conformations. Both structures are calculated to be true local minima on the potential energy surface. The energy difference between the two conformations is very small, 0.1 kcal mol⁻¹. Kaliannan et al. have attempted to rationalize the conformational preference exhibited by the neutral acid form in terms of the interaction of polar bonds and the dipoles on the atoms.[6] In both **2a** and **2b**, the N–S bond lengths, 1.633 and 1.610 Å, respectively, are considerably shorter (by ~0.3 Å) than those in the zwitterions (**1a** and **1b**). These shorter N–S bond lengths can be attributed to the overlap of the nitrogen p orbital with sulfur 3d orbitals. However, no empty p orbital is available for such a π orbital in the zwitterion.

The calculated energy difference between the zwitterion (**1a**) and the neutral form (**2a**) (Table IV) is quite dependent on the theoretical level employed. At the Hartree–Fock levels, **2a** is more stable than **1a** by 3–6 kcal mol⁻¹. Inclusion of p-polarization functions on hydrogen has significant effect on the relative energy (by 2.2 kcal mol⁻¹), whereas inclusion of f functions on heavy atoms and expansion of basis set from double-ζ valence to triple-ζ valence have little effect. Incorporation of electron correlation lowers the energy of the zwitterionic form more than the neutral. At the MP2/6-31+G(2d,p) level, the zwitterion is favored over the neutral by 1.7 kcal mol⁻¹, but higher treatments of electron correlation (MP3, MP4SDQ, QCISD) have a less dramatic effect on the relative energies. At the QCISD/6-31+G(2d,p) level, the neutral is favored by 0.8 kcal mol⁻¹. Inclusion of triple substitution in the MP4SDQ and QCISD theories with the smaller 6-31G(d) basis set is also found to have significant effect on the energy difference, 1.1 kcal mol⁻¹ in favor of the zwitterion. Including this effect of triple substitution, the zwitterion is more stable than the neutral form by 0.4 kcal mol⁻¹. Zero-point vibrational energy correction at the HF/6-31+G(2d) level favors the neutral by 0.8 kcal mol⁻¹. Hence, our final best estimate is that the neutral is favored by 0.5 kcal mol⁻¹.

Finally, we consider the rearrangement process of **1a** to **2a**. The interconversion of **1a** and **2a** is possible through a hydrogen 1,3-shift, via transition structure **3**. The calculated barrier height for this rearrangement is 28.6 kcal mol⁻¹. Neglect of electron correlation leads to a significantly larger barrier of 39.7 mol⁻¹. Note that the transition structure (**3**) has a hydrogen bridged between the sulfur and oxygen atoms. Thus, we conclude that both the zwitterion and neutral form are very close in energy and experimentally observable in the gas phase. This result is in contrast to the strong preference of the neutral form calculated for glycine and other amino acids in the gas phase.[22] The zwitterionic forms of these amino acids are 20–60 kcal mol⁻¹ higher in energy than the corresponding neutral forms.[22]

## Structures and Energies in Condensed Media

The calculated dipole moments of **1a** and **2a** at the MP2/6-31+G(2d,p) level are 6.62 and 3.56 D, respectively. Therefore, one would expect a substantial differential stabilization effect in condensed media. In a nonpolar medium ($\epsilon = 2.0$), the zwitterion is calculated to have a larger stabilization energy (5.1 kcal mol⁻¹) than the neutral form (2.0 kcal mol⁻¹). Thus, the zwitterion is predicted to be the dominant form in nonpolar media. The differential stabilization effect is even more pronounced in a polar medium of $\epsilon = 40.0$; the zwitterion is more stable than the neutral form by 10.2 kcal mol⁻¹. There is a substantial enhancement of the dipole moment (by 3.1 D) of **1a** on going from the gas phase

(19) (a) Oh, J. J.; LaBarge, M. S.; Matos, J.; Kampf, J. W.; Hillig II, K. W.; Kuczkowski, R. L. *J. Am. Chem. Soc.* **1991**, *113*, 4732. (b) LaBarge, M. S.; Matos, J.; Hillig II, K. W.; Kuczkowski, R. L. *J. Am. Chem. Soc.* **1987**, *109*, 7222.

(20) Bühl, M.; Steinke, T.; Schleyer, P. v. R.; Boese, R. *Angew. Chem.*, in press.

(21) Thorne, L. R.; Suenram, R. D.; Lovas, F. J. *J. Chem. Phys.* **1983**, *78*, 167.

(22) (a) Tse, Y. C.; Newton, M. D.; Vishveshwara, S.; Pople, J. A. *J. Am. Chem. Soc.* **1978**, *100*, 4329. (b) Wright, L. R.; Borkman, R. F. *J. Am. Chem. Soc.* **1980**, *102*, 6207. (c) Voogd, J.; Derissen, J. L.; Van Dujineveldt, F. B. *J. Am. Chem. Soc.* **1981**, *103*, 7701. (d) Bonaccorsi, R.; Palla, P.; Tomasi, J. *J. Am. Chem. Soc.* **1984**, *106*, 1945. (e) Kikuchi, O.; Natsui, T.; Kozaki, T. *J. Mol. Struct.* (*Theochem*) **1990**, *207*, 103.

to a polar medium. Thus, our computational results agree with the experimental finding that sulfamic acid exists predominantly in the zwitterionic form in condensed media.

Although the energy difference between the gauche (**2a**) and anti (**2b**) conformations of the neutral form is small in the gas phase, the gauche conformer is predicted to have a large stabilization energy in a polar medium. In a medium of $\epsilon = 40.0$, the gauche conformer is 1.7 kcal mol$^{-1}$ lower in energy than the anti form. The rearrangement process from the neutral (**2a**) to the zwitterion (**1a**) is predicted to have a smaller barrier (24.3 kcal mol$^{-1}$) in a polar medium. On going from the gas phase to a polar medium, there is a substantial increase (19.1–32.6 kcal mol$^{-1}$) in the energy for the dissociation process $^+H_3NSO_3^-$ (**1a**) $\rightarrow$ NH$_3$ + SO$_3$. Thus, the reaction of NH$_3$ with SO$_3$ to form sulfamic acid should be a more favorable process in a polar medium.

As with the staggered conformation (**1a**), the N–S bond length of the eclipsed conformation (**1b**) of the zwitterion is also reduced remarkably (by 0.114 Å) on going from vacuo to a condensed medium (Figure 1). For the anti conformation of the neutral form (**2b**), the introduction of a dielectric medium seems to have little effect on the calculated geometry. On the other hand, large structural changes are observed for the gauche conformation (**2a**). For instance, the H$_1$O$_1$SO$_3$ torsional angle increases 24.3° on going from the gas phase to a polar medium. Interestingly, the optimized N–S bond lengths of both the anti and gauche conformations of **2** in a polar medium are the same (1.608 Å), in spite of their substantial difference in N–S bond length (0.023 Å) in the gas phase.

## Charge Distributions and Topological Properties

As pointed out by a previous Morokuma component analysis of the energetics of the complex formation between NH$_3$ and SO$_3$, the electrostatic and charge-transfer terms are the main contributions to the interaction energy.[5e] This is readily confirmed by electron populations calculated from Bader's theory of atoms in molecules.[16] The atomic charges, given by the nuclear charges less the electron populations, are shown in Figure 2. The zwitterion (**1a**) shows a large amount of charge transfer (0.28e) from the NH$_3$ group to the SO$_3$ moiety. In a polar medium, the degree of charge transfer (0.36e) is even more pronounced. As may be expected, the hydrogens become more positive and the oxygens more negative. In other words, a stronger zwitterionic character is developed in the presence of the solvent reaction field. This stronger effect of charge transfer from NH$_3$ to SO$_3$ is also reflected in the increase of OSN bond angle from the gas phase (97.8°) to a polar medium (101.0°) (Figure 1). Interestingly, the O–S–N–H skeleton displays an alternating charge distribution, with all atoms bearing relatively strong charges (Figure 2). In particular, the charges of the oxygens and hydrogens are considerably larger than the corresponding atoms in the NH$_3$ and SO$_3$ monomers. It thus appears that the stabilization of the S–N bond in the zwitterion is in part due to the strong electrostatic attraction. This leads to an intriguing question concerning the nature of the N–S bond. Is the N–S bond covalent or ionic? The nature of atomic interactions can be examined by considering the topological properties at the bond critical point. It has been shown that the investigation of the Laplacian ($\nabla^2 \rho_b$) and local energy density ($H_b$) provides useful means to distinguish between covalent bonds and closed-shell interactions.[23,24] The sign of the Laplacian electron density ($\nabla^2 \rho_b$) indicates whether there is a local concentration ($\nabla^2 \rho_b < 0$) or a local depletion ($\nabla^2 \rho_b > 0$) of charge.[23] The local energy density ($H_b$) is defined as the sum of the local potential energy density ($V_b$) and local kinetic energy density ($G_b$). Since $V_b$ is always negative and $G_b$ is always positive, the sign of $H_b$ reveals whether the accumulation of electron density at the bond critical point is stabilizing ($H_b < 0$) or destabilizing ($H_b > 0$).

For a covalent bond, the local energy density at the bond critical point is always negative (stabilizing).[24] From Table V, we see that the N–S bond of the zwitterion exhibits the characteristics of a covalent interaction. At the bond critical point, $\nabla^2 \rho_b < 0$ and $H_b < 0$; i.e., both the electrostatic and energetic aspects of a shared interaction are satisfied. Stronger covalent character is predicted for the N–S bond in a condensed medium. The calculated covalent bond order increases significantly, from 0.46 to 0.58. In order to separate the influence of the reaction field from the effect of the geometry change on the charge density, an SCRF calculation on the unrelaxed (gas-phase) geometry was performed. In this case, the changes in $\rho_b$, $\nabla^2 \rho_b$, and $H_b$ are in the same direction as those found for the fully relaxed SCRF geometry, but with smaller magnitudes. The change in electron density in the presence of a reaction field is shown pictorially in Figure 4. This shows the transfer of electron density from the amino hydrogens to the SO$_3$ oxygens, as seen in the atomic charges (Figure 2).

It is interesting to compare the topological properties of the B–N bond critical point of BH$_3$·NH$_3$, another example of strong donor–acceptor complex, with the N–S bond critical point of **1a**. The B–N bond in the amine–borane complex is found to be dominated by ionic interaction. This is manifested by a smaller $\rho_b$ and a positive $\nabla^2 \rho_b$ (Table V). In addition, the local energy density ($H_b$) is closer to zero. The calculated covalent bond order is just 0.26. The calculated charge transfer (0.09e) in the BH$_3$·NH$_3$ complex is significantly smaller than that in the zwitterion of sulfamic acid. These results suggest that the interaction of BH$_3$ with NH$_3$ to form BH$_3$·NH$_3$ is dominated by electrostatic attraction, with a relatively smaller contribution from charge transfer. However, a larger binding energy of 28.7 kcal mol$^{-1}$ is predicted for this donor–acceptor complex.[25]

For the neutral form (**2a**) of sulfamic acid, the changes in atomic charge are smaller than those in the zwitterion (**1a**). The largest changes occur in the hydrogens of the amine group. In accordance with the shorter N–S bond length, greater covalent character is found for the N–S bond in **2a**. This is reflected by the greater magnitude of $\rho_b$, $\nabla^2 \rho_b$, and $H_b$, as compared to the corresponding values in **1a** (Table V). Significant bond ellipticity is also calculated for the N–S bond in **2a**. This confirms the $\pi$ interaction in this bond. As with the zwitterion, stronger covalent character is developed in condensed medium. However, there is a slight decrease in the $-\nabla^2 \rho_b$ value in this case. Interestingly, the changes in the topological properties evaluated with the gas-phase geometry are greater than those computed with the SCRF geometry. In summary, the presence of a polar dielectric medium leads to stronger covalent interaction in the N–S bond and favors larger charge separation for both the zwitterionic and neutral forms.

## Vibrational Frequencies and Infrared Spectra

To facilitate future characterization of **1a** and **2a** in the gas phase, we have reported the complete set of calculated harmonic frequencies (Tables VI and VII) and their computed infrared spectra (Figure 4). First, we note that the presence of a dielectric medium has a strong influence on the calculated vibrational frequencies. As evident in Table VI, there are striking changes in the calculated frequencies of **1a** on going from the gas phase to a polar medium ($\epsilon = 40.0$). Large frequency shifts (above 50 cm$^{-1}$) are observed in $\nu_1$, $\nu_2$, $\nu_5$, $\nu_7$, $\nu_9$, and $\nu_{10}$. The largest frequency shift, 142 cm$^{-1}$, corresponds to the N–S stretching frequency ($\nu_5$). Significant changes in frequencies are also observed in the neutral form (**2a**). For example, there is massive change in vibrational frequency, by 201 cm$^{-1}$, in the N–S vibrational mode ($\nu_{11}$). These changes are partly due to the large change in geometry and partly due to the presence of the solvent reaction field.

The infrared and Raman spectra of the zwitterion in the solid state have been reported.[26] Detailed assignments of the observed

(23) (a) Bader, R. F. W.; Essen, H. *J. Chem. Phys.* **1984**, *80*, 1943. (b) Bader, R. F. W.; MacDougall, P. J.; Lau, C. D. H. *J. Am. Chem. Soc.* **1984**, *106*, 1594.

(24) (a) Cremer, D.; Kraka, E. *Angew. Chem., Int. Ed. Engl.* **1984**, *23*, 627. (b) Cremer, D.; Kraka, E. *Croat. Chem. Acta* **1984**, *57*, 1265. (c) Cremer, D.; Kraka, E. *J. Am. Chem. Soc.* **1985**, *107*, 3800.

(25) Binkley, J. S.; Thorne, L. R. *J. Chem. Phys.* **1983**, *79*, 2932.

(26) (a) Nakagawa, I.; Mizushima, S. I.; Saraceno, J.; Lane, T. J.; Quagliano, J. V. *Spectrochim. Acta* **1958**, *12*, 239. (b) Vuagnat, A. M.; Wagner, E. L. *J. Chem. Phys.* **1957**, *26*, 77.

spectrum have been made with the aid of normal-coordinate analysis.[26] Vibrational frequencies calculated at the Hartree–Fock level are known to be an average ~10% greater than the experimental frequencies for a wide range of molecules,[27] and therefore the frequencies calculated here are scaled by 0.9 for comparison with experiments. If one compares the set of scaled gas-phase frequencies with the solid-state experimental values, the agreement is significantly worse than one might have expected at that level of theory. However, vibrational frequencies calculated in a polar medium are in substantially better agreement. In particular, the deviations between theory and experiment for the $\nu_2$, $\nu_5$, and $\nu_{10}$ vibrational frequencies are reduced from 119, 188, and 159 cm$^{-1}$, respectively, to 16, 61, and 79 cm$^{-1}$.

Another interesting aspect related to the changes in vibrational frequencies is the assignment of vibrational modes. The assignments for the gas-phase and SCRF vibrational frequencies are the same except for the $\nu_4$ and $\nu_5$ absorption modes. These two bands are mixtures of N–S stretch and symmetric SO$_3$ deformation modes. In the gas phase, the $\nu_4$ band is dominated by the N–S stretch, whereas in a polar medium it is predominantly an SO$_3$ deformation. The situation is exactly reversed for the $\nu_5$ absorption peak. Therefore, the assignment of $\nu_5$ (604 cm$^{-1}$) to the N–S stretch is consistent with the experimental assignment.[26] However, smaller value ($\nu_4 = 345$ cm$^{-1}$) is predicted for N–S stretching frequency in the gas phase.

Figure 4 displays the calculated IR spectra of both the zwitterion (**1a**) and neutral form (**2a**) in the gas phase and polar medium. It is immediately apparent that the calculated IR intensities are substantially different. In general, most absorption peaks are more intense on going from vacuum to a polar medium, and the ratios of increase are about the same. Note that some decreases in intensity are observed. For instance, the intensity of the $\nu_4$ absorption peak of the zwitterion is calculated to decrease significantly from 61 to 14 km mol$^{-1}$.

**Conclusions**

Several interesting points have been revealed by this study:

(1) In the gas phase, the zwitterionic form (staggered $C_{3v}$, **1a**) of sulfamic acid lies within 1 kcal mol$^{-1}$ of the neutral acid form

(gauche-HOSN $C_1$, **2a**). These two structures are separated by a barrier of 28.6 kcal mol$^{-1}$. Correction for electron correlation is essential in evaluating the relative stability of the zwitterion and neutral isomers.

(2) The binding energies of the zwitterion, relative to ammonia and sulfur trioxide, in the gas phase and in a polar medium are 19.1 and 32.6 kcal mol$^{-1}$, respectively. The N–S bond of the zwitterion exhibits characteristics of a shared interaction. Stronger covalent character is predicted for this N–S bond than the B–N bond of BH$_3$·NH$_3$.

(3) In agreement with experiment, the zwitterion is calculated to be the preferred structure in both nonpolar and polar condensed media. In a dielectric medium of $\epsilon = 40.0$, the zwitterion is significantly more stable than the neutral form by 10.2 kcal mol$^{-1}$. On going from the gas phase to a polar medium, significant enhancement of the dipole moment (by 3 D) of the zwitterion is observed. Stronger covalent character is also predicted for the N–S bond.

(4) The discrepancy between the calculated and solid-state geometries of the zwitterion (**1a**), reported by Hickling and Woolley, has been resolved. It is the result of a genuine difference in structure between the gas phase and solid state. The N–S bond length is calculated to decrease by 0.10 Å from the gas phase to a dielectric medium of $\epsilon = 40.0$, and the OSN angle is calculated to increase by 3°.

(5) The infrared spectra of both **1a** and **2a** are strongly influenced by the solvent reaction field. Large frequency shifts (up to 200 cm$^{-1}$ and intensity changes are observed. The calculated frequencies are in better agreement with the solid-state experimental data when the reaction field is included.

(6) All the results, including the geometry changes, the changes in relative energies, and the changes in vibrational frequencies from gas phase to a polar medium, are in good accord with the experimental findings. This demonstrates that the reaction field model provides an adequate description of a compact dipolar molecule in any polarizable environment.

(27) Pople, J. A.; Schlegel, H.; Krishnan, R.; DeFrees, D. J.; Binkley, J. S.; Frisch, J. A.; Whiteside, R. F.; Hout, R. F.; Hehre, W. J. *Int. J. Quantum Chem. Symp.* **1981**, *15*, 269.

---

# Determination of Enantiomerization Barriers by Computer Simulation of Interconversion Profiles: Enantiomerization of Diaziridines during Chiral Inclusion Gas Chromatography

**M. Jung and V. Schurig***

*Contribution from the Institut für Organische Chemie der Universität, Auf der Morgenstelle 18, D-7400 Tübingen, Germany. Received May 20, 1991*

**Abstract:** A new general computer program has been developed for the simulation of chromatograms featuring dynamic phenomena in chromatography. It has been applied to the determination of enantiomerization barriers by simulation of experimentally observed elution profiles of enantiomers interconverting during their separation on a chiral stationary phase in a chromatographic column. For two diaziridines interconversion profiles could be observed in inclusion gas chromatography using permethylated $\beta$-cyclodextrin dissolved in OV-1701 as stationary phase. The simulation obtained at different temperatures and pressures yielded $\Delta G^*_s$ in the stationary phase 1–4 kJ/mol lower than $\Delta G^*_m$ in the mobile phase. From the temperature dependence of $\Delta G^*_s$, the quantities $\Delta H^*_s$ and $\Delta S^*_s$ in the stationary phase have been determined. Furthermore, the concept of the retention increase $R'$ (caused by the addition of the cyclodextrin to the achiral polysiloxane OV-1701) allowed a separation of the contributions of enantiomerization in the physically dissolved state on the one hand and in the complexed state of the enantiomers on the other hand to the overall enantiomerization barrier in the stationary phase, $\Delta G^*_s$.

In analogy to dynamic NMR spectroscopy,[1] dynamic chromatography has been introduced in recent years as a tool for the

investigation of dynamic processes[2] and the determination of the corresponding rate constants[3-5] and has been applied to the in-